Robust Optimal Control of Polymorphic Transformation in Batch Crystallization

Martin Wijaya Hermanto and Min-Sen Chiu
Dept. of Chemical and Biomolecular Engineering, National University of Singapore, Singapore 117576

Xing-Yi Woo
Dept. of Chemical and Biomolecular Engineering, National University of Singapore, Singapore 11576; and Dept. of Chemical and Biomolecular Engineering, University of Illinois at Urbana-Champaign, IL 61801

Richard D. Braatz
Dept. of Chemical and Biomolecular Engineering, University of Illinois at Urbana-Champaign, IL 61801

DOI 10.1002/aic.11266
Published online August 27, 2007 in Wiley InterScience (www.interscience.wiley.com).

One of the most important problems that can arise in the development of a pharmaceutical crystallization process is the control of polymorphism, in which there exist different crystal forms for the same chemical compound. Different polymorphs can have very different properties, such as bioavailability, which motivates the design of controlled processes to ensure consistent production of the desired polymorph to produce reliable therapeutic benefits upon delivery. The optimal batch control of the polymorphic transformation of L-glutamic acid from the metastable α-form to the stable β-form is studied, with the goal of optimizing batch productivity, while providing robustness to variations in the physicochemical parameters that can occur in practice due to variations in contaminant profiles in the feedstocks. A nonlinear state feedback controller designed to follow an optimal setpoint trajectory defined in the crystallization phase diagram simultaneously provided high-batch productivity and robustness, in contrast to optimal temperature control strategies that were either nonrobust or resulted in long-batch times. The results motivate the incorporation of the proposed approach into the design of operating procedures for polymorphic batch crystallizations. © 2007 American Institute of Chemical Engineers *AIChE J,* 53: 2643–2650, 2007

Keywords: T-control, robust T-control, C-control, polymorphic transformation, pharmaceutical crystallization

Introduction

Polymorphism, in which multiple crystal forms exist for the same chemical compound, is of significant interest to the pharmaceutical industry.[1–5] According to Ostwald's Rule of Stages, in a polymorphic system, the most soluble metastable form appears first, followed by more stable polymorphs. This rule holds for most polymorphic systems, which implies that care must be taken to avoid the formation of metastable crystals when trying to crystallize the most stable crystal form. Sometimes a relatively small shift in the operating conditions can result in the appearance of crystals of an undesired polymorph.

Metastable crystals have appeared during the production of specialty chemicals, such as pharmaceuticals, dyestuffs, and pesticides. The variation in physical properties, such as crystal shape, solubility, hardness, color, melting point, and chemical reactivity makes polymorphism an important issue for the food, specialty chemical, and pharmaceutical indus-

Correspondence concerning this article should be addressed to Min-Sen Chiu at checms@nus.edu.sg.

tries, where products are specified not by chemical composition only, but also by their performance.[2] As a result, controlling polymorphism to ensure consistent production of the desired polymorph is important in those industries, including the drug manufacturing industry where safety is paramount. Deliberate isolation of metastable phases is sometimes desired when they have advantageous processing or application properties, such as increased dissolution rate. In most cases, however, the formulation of a product as a metastable phase is undesired due to potential subsequent phase transformation during drying or storage, which would change product characteristics.[6]

Although the crystallization control literature is vast, to the authors' knowledge there are no articles on the optimal control of crystallization processes in which more than one polymorph occurs. The vast majority of articles on nonpolymorph crystallization have considered the optimal control of only one or two characteristics of the crystal-size distribution, such as weight mean size. The most widely studied approach is to determine a temperature profile (T-control) that optimizes an objective function based on an offline nominal model.[7–11] Although T-control is simple to implement, it has become well-known in recent years that T-control can be very sensitive to variations in the kinetic parameters.[12,13] This motivated the development of robust T-control, which explicitly includes the impact of uncertainties in the objective, while determining the optimal temperature-time trajectory to be followed during batch operation.[14–16] With advances in sensor technologies, another control strategy developed to provide improved robustness to model uncertainty is C-control, which follows an optimal or nearly optimal concentration-temperature trajectory.[3,13,17–19]

Motivated by the industrial need to control polymorphism,[2,20] this article evaluates and compares the performance of these optimal control strategies for the polymorphic transformation of L-glutamic acid from the metastable α-form to the stable β-form. The Process Description section describes the process model for the polymorphic transformation of L-glutamic acid. The T-control, robust T-control, and C-control sections discuss the three control strategies investigated in this article. The simulation results in the Results section are followed by the conclusions.

Process Description

The population balance equations for the polymorphic transformation of L-glutamic acid from the metastable α-form to the stable β-form are[21]:

$$\frac{\partial f_\alpha}{\partial t}+\frac{\partial (D_\alpha f_\alpha)}{\partial L}=0, \tag{1}$$

$$\frac{\partial f_\beta}{\partial t}+\frac{\partial (G_\beta f_\beta)}{\partial L}=B_\beta \delta(L-L_0), \tag{2}$$

where

$$f_\alpha^0(L)=f_\alpha(L,0), \tag{3}$$

$$D_\alpha = k_{d,\alpha}\frac{(C-C_{sat,\alpha})}{100} \quad (\alpha\text{-dissolution rate}), \tag{4}$$

$$G_\beta = k_{g,\beta}L\frac{(C-C_{sat,\beta})}{100} \quad (\beta\text{-growth rate}), \tag{5}$$

$$C_{sat,i}=a_i\exp(b_iT), \quad i\in\{\alpha,\beta\} \quad (\text{solubilities}), \tag{6}$$

$$k_{d,\alpha}=\exp\left(\frac{8.9870\times10^7}{T^2}-\frac{6.0761\times10^5}{T}+1.0141\times10^3\right), \tag{7}$$

$$k_{g,\beta}=0.410\exp\left(-\frac{10900}{8.314\,T}\right). \tag{8}$$

f_i is the number density for the i-form crystals. The initial crystal-size distributions of polymorph i, $Y_i(L,0)$, is described by the sum of three log-normal distributions, the n^{th} moment of the i-form crystals is

$$\mu_{i,n}=\int_0^\infty L^n f_i dL, \tag{9}$$

and the nucleation rate for β-form crystals is

$$B_\beta = k_{b,\beta}\frac{(C-C_{sat,\beta})}{100}\mu_{\beta,3}, \tag{10}$$

$$k_{b,\beta}=7\times10^7. \tag{11}$$

Applying the method of characteristics to Eq. 1, and method of moments to Eq. 2, gives

$$f_\alpha(L,t)=f_\alpha^0\left(L-\int_0^t D_\alpha dt\right), \quad L\geq 0 \tag{12}$$

$$\frac{d\mu_{\beta,n}}{dt}=nG'_\beta\mu_{\beta,n}+B_\beta L_0^n, \quad n=0,1,2,... \tag{13}$$

where $G'_\beta = G_\beta/L$. The aforementioned equations are augmented by the solute mass balance:

$$\frac{dC}{dt}=-300\frac{\rho_c V_{slurry}}{m_{solution}}\left(1-\frac{C}{100}\right)\left(k_{v,\alpha}D_\alpha\mu_{\alpha,2}+k_{v,\alpha}\frac{D_\alpha f_\alpha(L_0,t)L_0^3}{3}+k_{v,\beta}G'_\beta\mu_{\beta,3}+k_{v,\beta}\frac{B_\beta L_0^3}{3}\right), \tag{14}$$

where ρ_c is the crystal density, $m_{solution}$ is the mass of solution, V_{slurry} is the total volume of crystals and solution, $k_{v,i}$ is the volumetric shape factor for polymorphic form i, and L_0 is the size of the nucleated crystals. The parameter values are in Ref. 21. In this study, the following uncertain parameters are assumed:

$$k'_{g,\beta}=k_{g,\beta}(1+\theta_1)\exp\left(-\frac{10900}{8.314T}\theta_2\right), \quad -0.2\leq\theta_1,\theta_2\leq0.2 \tag{15}$$

$$k'_{d,\alpha}=k_{d,\alpha}(1+\theta_3), \quad -0.2\leq\theta_3\leq0.2 \tag{16}$$

$$C'_{sat,\alpha}=C_{sat,\alpha}(1+\theta_4), \quad -0.05\leq\theta_4\leq0.05 \tag{17}$$

$$C'_{sat,\beta}=C_{sat,\beta}(1+\theta_5), \quad -0.05\leq\theta_5\leq0.05 \tag{18}$$

where θ_1 and θ_2 are the uncertainties in the growth parameters for the β-form crystals, θ_3 is the uncertainty in the dissolution kinetics of the α-form crystals, and θ_4 and θ_5 are the uncertainties in the solubility curves of the α and β forms, respectively. The nominal model corresponds to $\theta_i = 0$, $i = 1,\ldots,5$. While uncertainties in parameters quantified from

experimental data are typically correlated,[22,23] uncorrelated uncertainties were used here so as to separately assess the robustness to different types of uncertainties.

T-control

The first journal articles on the control of batch polymorphic crystallization implemented temperature control (e.g., see[21]). The most widely studied approach for the optimal control of nonpolymorphic crystallization processes has utilized T-control, in which the temperature trajectory has been computed from the optimization of an objective function, based on an offline model with nominal parameters.[9] In this study, the objective function that is maximized is the yield of the β-form minus a penalty on the time required for the mass of the α-form to be below some tolerance

$$\begin{aligned} I_{nominal} &= m_\beta(t_f) - w_n t_\alpha(\gamma) \\ &= \rho_c k_{v,\beta} V_{slurry} \mu_{\beta,3}(t_f) - w_n t_\alpha(\gamma) \end{aligned} \tag{19}$$

where t_f is the batch time, $m_\beta(t_f)$ is the yield of β-form at the end of the batch, $t_\alpha(\gamma)$ is the time taken to reduce the mass of α-form below γ, and w_n is a weighting parameter. The values of t_f, w_n, and γ are 7 h, 1×10^{-3}, and 5×10^{-4} g, respectively. The second term $t_\alpha(\gamma)$ is included to increase the productivity of the batch crystallizer (shorter batch times lead to more batches per day).

To implement this strategy, the temperature-time trajectory is parameterized as a first-order spline with 64 time intervals (6.56 min). Examination of the temperature trajectories indicated that this temporal resolution is fine enough for this crystallization process. The temperature trajectory was constrained to be within the region where crystals of the α-form dissolve, while crystals of the β-form grow, that is, the temperature is constrained to be between the saturation temperatures of the α- and β-forms ($T_{sat,\alpha} \le T \le T_{sat,\beta}$).* In addition, the minimum and maximum temperature can be achieved by cooling and heating are 25°C and 50°C. These constraints were handled by parameterizing the temperature-time trajectory, such that the decision variables were fractions between 0 and 1, with 0 and 1 indicating the lower and upper bounds on the temperature at each time instance, respectively. A genetic algorithm was used to determine an initial temperature trajectory, which was further optimized using sequential quadratic programming. The resulting concentration-temperature trajectory for nominal model is shown in Figure 1. There are two sections in the trajectory (heating followed by cooling) where the supersaturation of β-form is maximized due to its growth kinetics being the rate-limiting step.

Robust T-control

The solubility curves and nucleation and growth kinetics can vary somewhat from batch to batch due to impurities in the feed. Further, any model parameters obtained from experiments have uncertainties due to measurement noise and unmeasured disturbances that occur during the collection of the experimental data used to estimate parameters. Assuming all the uncertainties are independent from each other,

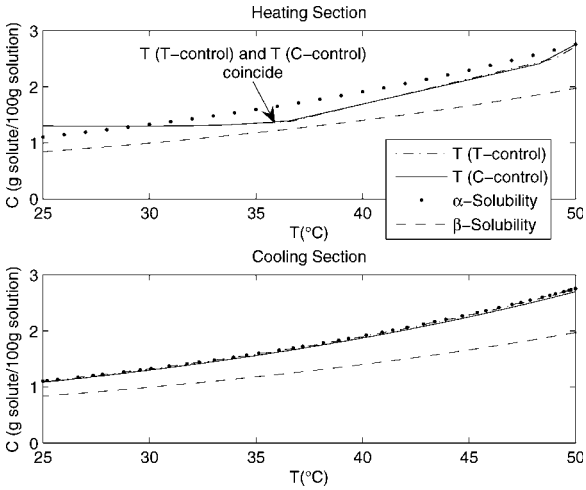

Figure 1. Solubility curves and concentration-temperature trajectories of T-control and C-control with parameters p_1 = 36.56, p_2 = 11.5, p_3 = 0.4340, and p_4 = 0.03656.

$$\theta_{min,i} \le \theta_i \le \theta_{max,i}, \tag{20}$$

the uncertain parameters may be expressed as:

$$\varepsilon_\theta = \left\{ \theta : \theta = \hat{\theta} + \delta\theta, \|\mathbf{W}_\theta \delta\theta\|_\infty \le 1 \right\}, \tag{21}$$

$$\hat{\theta} = \frac{\theta_{min} + \theta_{max}}{2}, \tag{22}$$

$$(\mathbf{W}_\theta)_{jj} = \frac{2}{\theta_{max,j} - \theta_{min,j}}, \tag{23}$$

where $\theta = [\theta_1, \theta_2, \ldots, \theta_n]^T$, $\hat{\theta} = [\hat{\theta}_1, \hat{\theta}_2, \ldots, \hat{\theta}_n]^T$, $\theta_{min} = [\theta_{min,1}, \theta_{min,2}, \ldots, \theta_{min,n}]^T$, and $\theta_{max} = [\theta_{max,1}, \theta_{max,2}, \ldots, \theta_{max,n}]^T$ are the actual, nominal, minimum, and maximum values of the uncertain model parameters, respectively, $\mathbf{W}_\theta$ is a weight matrix quantifying the magnitude of the uncertainty in each parameter, and $\| \cdot \|_\infty$ is the vector ∞-norm.

In robust T-control the objective function to be maximized appends a term to include the impact of uncertain parameters[14–16]

$$I_{robust} = I_{nominal} - w_r \delta I_{w.c} \tag{24}$$

where $w_r \in [0,1]$ is a weighting parameter and $\delta I_{w.c.}$ is the worst-case deviation in the objective due to model uncertainties. If $w_r = 1$, I_{robust} is the objective function obtained for the worst-case perturbation at the cost of potential degradation in nominal performance. The value of w_r can be selected to be smaller than one depending on the desired trade-off between the nominal and worst-case performance. In this paper, $w_r = 0.6$ provided the best balance between nominal and worst-case performance. In robust T-control the objective (24) is maximized subject to the condition that the constraints in the previous section hold for all parameters within the uncertainty description.

*Note that a slight violation of this constraint occurs initially due to the initial concentration being outside this range. According to Ref. 21 the α-form crystals grow for a short time before crossing the α solubility curve.

With the widely-used approximation[22,24,25]

$$\delta I = \frac{\partial I}{\partial \theta}\delta\theta = \mathrm{L}\delta\theta, \tag{25}$$

where $\mathbf{L}$ is the objective function sensitivity row vector, the worst-case deviation in the objective function is[15,23]

$$\max_{\|\mathbf{W}_\theta \delta\theta\|_\infty \le 1} |\delta I| = \|\mathbf{L}\mathbf{W}_\theta^{-1}\|_1 \tag{26}$$

and a worst-case parameter uncertainty vector is

$$\delta\theta_{w.c} = \pm\mathbf{W}_\theta^{-1}\mathrm{v}, \text{ with } v_k = \frac{(\mathbf{L}\mathbf{W}_\theta^{-1})_k}{|(\mathbf{L}\mathbf{W}_\theta^{-1})_k|} = \text{ sgn } (\mathbf{L}\mathbf{W}_\theta^{-1})_k, \tag{27}$$

where $\| \cdot \|_1$ is the vector 1-norm and the objective function sensitivity vector can be computed from

$$\mathbf{L} = \left.\frac{\delta I}{\delta\theta}\right|_{t_f} = \left.\frac{\delta I}{\delta \mathbf{x}}\right|_{t_f}\left.\frac{\delta \mathbf{x}}{\delta\theta}\right|_{t_f} = \begin{bmatrix}\frac{\partial I}{\partial x_1} & \frac{\partial I}{\partial x_2} & \cdots & \frac{\partial I}{\partial x_n}\end{bmatrix}\begin{bmatrix}\frac{\partial x_1}{\partial\theta_1} & \frac{\partial x_1}{\partial\theta_2} & \cdots & \frac{\partial x_1}{\partial\theta_p} \\ \frac{\partial x_2}{\partial\theta_1} & \frac{\partial x_2}{\partial\theta_2} & \cdots & \frac{\partial x_2}{\partial\theta_p} \\ \vdots & \vdots & \ddots & \vdots \\ \frac{\partial x_n}{\partial\theta_1} & \frac{\partial x_n}{\partial\theta_2} & \cdots & \frac{\partial x_n}{\partial\theta_p}\end{bmatrix} \tag{28}$$

where $\mathrm{x} = [x_1, x_2, \ldots, x_n]^T$ is the vector of the states involved in the simulation; for this study,

$$\mathrm{x} = [\mu_{\alpha,0}, \mu_{\alpha,1}, \mu_{\alpha,2}, \mu_{\alpha,3}, \mu_{\alpha,4}, \mu_{\beta,0}, \mu_{\beta,1}, \mu_{\beta,2}, \mu_{\beta,3}, \mu_{\beta,4}, C, h]^T \tag{29}$$

with $h = \int_0^t D_\alpha(\tau)d\tau$.

The system Eqs. 9, 12, 13, and 14 can be represented as a system of differential-algebraic equations (DAE):

$$\mathbf{M}\dot{\mathbf{x}} = \mathbf{f}(t, \mathbf{x}; \theta) \tag{30}$$

where $\mathbf{M}$ is an $n \times n$ mass matrix of constant coefficients of the form

$$\mathbf{M} = \begin{bmatrix}\mathbf{I}^{(s)} & 0 \\ 0 & 0^{(n-s)}\end{bmatrix} \tag{31}$$

and $\mathbf{I}^{(s)}$ is the $s \times s$ identity matrix, and $\mathbf{0}^{(n-s)}$ is the $(n - s) \times (n - s)$ matrix of zeroes. In this study, $s = 7$ and $n = 12$.

Differentiating the system equation with respect to θ gives the sensitivity equation

$$\mathbf{M}\frac{\partial\dot{\mathbf{x}}}{\partial\theta} = \frac{\partial\mathbf{f}}{\partial\mathbf{x}}\frac{\partial\mathbf{x}}{\partial\theta} + \frac{\partial\mathbf{f}}{\partial\theta}. \tag{32}$$

The following steps were used to compute the robust temperature profile:

(1) The first iteration ($j = 1$) was initialized with random parameters for the temperature profile. For $j > 1$, the temperature parameters were determined from a genetic algorithm applied to the optimization of the robust objective function subject to all operating constraints for the full range of uncertain parameters.

(2) The temperature profile from Step 1 was applied to the nominal model ($\theta_i = 0$ for $i = 1, \ldots, 5$) by integrating the system Eq. 30, and the sensitivity Eq. 32. At the final batch time (t_f), the nominal objective function ($I_{nominal}$) was obtained from Eq. 19.

(3) The objective function sensitivity vector ($\mathbf{L}$) was computed from Eq. 28, and the worst-case parameter uncertainties obtained from Eq. 27.

(4) The temperature profile from Step 1 was applied to the model with the worst-case model parameters calculated in Step 3. I_{robust} was calculated from Eq. 24 at the batch time t_f.

(5) Steps 1 to 4 were repeated until there was no significant change in the temperature profile.

This algorithm uses Eq. 25 only for estimating the worst-case parameters Eq. 27 with the full dynamic simulation used to compute I_{robust} (Step 4).

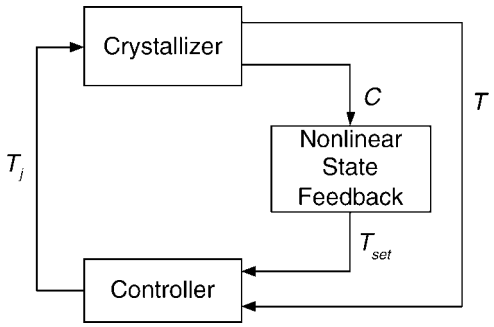

Figure 2. Prefered implementation of C-control for a batch cooling crystallizer.[26]

C-control

In many experimental and simulation studies of nonpolymorphic batch crystallizations, the C-control strategy (Figure 2) has resulted in low-sensitivity of the product quality to most practical disturbances and variations in kinetic parameters.[3,13,17–19,26] In the last two years, the C-control strategy has been applied experimentally to several polymorphic crystallizations, to produce large crystals of any selected polymorph.[27] C-control can be interpreted as nonlinear state feedback control,[26,28] in which the nonlinear master controller acts on the concentration C as a measured state[29] to produce the setpoint temperature T_{set} as its manipulated variable.[†] The difference between the calculated T_{set}, and the measured temperature T is used by the slave controller to manipulate the jacket temperature T_j, so that the deviation between T_{set} and T is reduced. Because the slave controller is just temperature control of a mixed tank, and the batch dynamics are relatively slow, any reasonably tuned proportional-integral controller will result in accurate following of T_{set}.

The setpoint concentration-temperature trajectory was parameterized as follows:

(1) Heating section:

(a) This time-dependent relation forces the temperature into the region between both solubility curves in the first 5.25 mins.

[†]For this application, the nonlinear master controller is given by Eqs. 35–38.

$$T' = T_o + \frac{p_1 - T_o}{(5.25)(60)} t \tag{33}$$

$$T_{set} = \max\{T_{min}, \min\{T', T_{max}\}\} \tag{34}$$

where p_1 (°C) is the first decision variable, $T_o = 25$°C is the initial temperature, $T_{min} = 25$°C and $T_{max} = 50$°C are the minimum and maximum temperatures achievable by cooling and heating the water bath, respectively, T_{set} is the setpoint temperature to a lower level controller, and t is time in seconds.

(b) Assuming a linear concentration-temperature trajectory when heating

$$T' = T_p + p_2(C - C_p) \tag{35}$$

$$T_{set} = \max(T_{min}, \min(T', T_{max})) \tag{36}$$

where $p_2\left(\frac{^\circ\text{C}}{\text{g solute}/100\text{ g solution}}\right)$ is the second decision variable, and T_p (°C) and C_p (g solute/100 g solution) are the temperature and concentration at time equal to 5.25 mins;

(2) Cooling section:

After the mass of α-form decreases below a certain value (chosen to be 0.5 g), the assumed trajectory is followed

$$T' = \frac{\ln(C/p_3)}{p_4} \tag{37}$$

$$T_{set} = \max(T_{min}, \min(T', T_{max})) \tag{38}$$

where p_3 (g solute/100 g solution), and p_4 (1/°C) are the third and fourth decision variables, respectively.

The rationale behind the structure of Eqs. 33 to 38 is to obtain the best fit to the concentration-temperature trajectory obtained by applying the optimal temperature-time trajectory from T-control to the nominal model. Then, the values for p_1 to p_4 were fitted accordingly. The lower level controllers for all control strategies are assumed to have very fast response compared to the overall batch time, which is a good assumption for this process, which has a relatively long batch time.

Results

This section compares the performance and robustness of the three control strategies to the parameter perturbations shown in Table 1. The yields and purities of β-form at the end of batch for all control strategies are tabulated in Table 2. The concentration-temperature trajectories in Figure 1 for T-control applied to the nominal model and the corresponding C-control obtained from Eqs. 33 to 38 are coincident, indicating that the parameterization of Eqs. 33 to 38, is suitable for representing the C vs. T setpoint used in C-control. The growth kinetics of the β crystals are relatively slow, which results in the optimal control trajectories being very close to the solubility curve for the α-form, to maximize the supersaturation with respect to the solubility of the β-form while operating between the two solubility curves.

The nominal temperature trajectory produced by T-control is highly nonrobust to perturbations in the physicochemical parameters, as seen in Figure 3b–d, with the temperature constraints violated for parameter sets 2 and 3. The temperature trajectories reoptimized for the perturbed model parameters indicate that the optimal temperature trajectory is very sensitive to shifts in the model parameters. The mass profiles in Figure 3e,f indicate that the crystals of the α-form completely dissolve within 2 h for the two feasible parameter sets, whereas crystals of the β-form continue to grow for 5 h, which is consistent with the notion that the growth rate of crystals of the β-form is rate-limiting for the design of the batch temperature trajectory for this polymorph transformation.

Table 1. Case 1 has no Uncertainties (the Nominal Model), Case 2 has the Worst-case Parameter Values, Case 3 is the same as Case 2, but only Includes Variations in the Kinetic Parameters, and Case 4 are Parameter Variations with Fast Growth Rate for Crystals of the β-form (Which is the Rate-limiting Step)

Cases	θ_1	θ_2	θ_3	θ_4	θ_5
1	0.0	0.0	0.0	0.0	0.0
2	−0.2	0.2	0.2	−0.05	0.05
3	−0.2	0.2	0.2	0.0	0.0
4	0.2	−0.2	0.2	−0.05	0.05

The temperature trajectories produced by robust T-control are robust in terms of satisfying the operating constraints for the whole set of perturbed parameters, but are very conservative in terms of having very long batch times, and poor productivity for all values of the physicochemical parameters (see Figure 4a–d). Comparing the reoptimized T-control and robust T-control mass profiles in Figure 4e,h indicates that robust T-control leads to unnecessarily long batch times for some values of the physicochemical parameters. Designing a batch control trajectory to satisfy the operating constraints for the whole set of potential perturbed model parameters can result in very sluggish performance irrespective of what the actual physicochemical parameters happen to be in a particular batch run. While such approaches have been heavily studied in the batch design and batch control literature (for example, see articles cited in[16]), these approaches can result in very poor performance when applied to practical batch processes.

Although C-control does not explicitly include robustness in its formulation, C-control nearly satisfies all of the operating constraints for all sets of model parameters (see Figure 5a–d), demonstrating nearly the same robustness as robust T-control.[‡] Further, C-control results in much faster batch times and higher productivity than robust T-control for some sets of physicochemical parameters (see Figure 5a and d). In addition, C-control results in the batch productivity similar to that obtained by T-control reoptimized for each parameter set, as seen by the closeness of the C-control and reoptimized T-control trajectories in Figure 5a–d. C-control has nearly the same performance as that of the best T-control trajectory, with the batch times obtained by C-control are large only when necessitated by the particular values of the physicochemical parameters. This performance is obtained by C-con-

[‡]There is a slight violation of the lower bound on temperature bound for the parameter set for Case 4, which is due to the shift in the solubility curve of the α-form. This violation can be removed by shifting the nominal concentration-temperature trajectory slightly away from the α-solubility curve (see Figure 6).

Table 2. The Yields and Purities of β-form at the End of Batch for Different Control Strategies

	Optimal		T-control		Robust T-control		C-control	
Cases	β-yield (g)	β-purity (%)	β-yield (g)	β-purity (%)	β-yield (g)	β-purity (%)	β-yield (g)	β-purity (%)
1	24.15	100.0	24.15	100.0	16.86	100.0	24.15	100.0
2	9.68	97.50	n.a.^	n.a.^	9.02	69.80	9.65	95.10
3	13.70	100.0	n.a.^	n.a.^	13.21	100.0	13.41	100.0
4	23.88	100.0	23.88*	100.0	16.42	100.0	n.a.†	n.a.†

^These values would be meaningless for comparison purposes due to temperature constraint violations.
*From Figure 3f, this value is approached at a much later time (4.67 h) compared to the optimal one (3 h).
†The constraint violation can be removed as mentioned in the text and Figure 6, and the resulting β-yield and purity are 23.86 g and 99.9%, respectively, for this case.

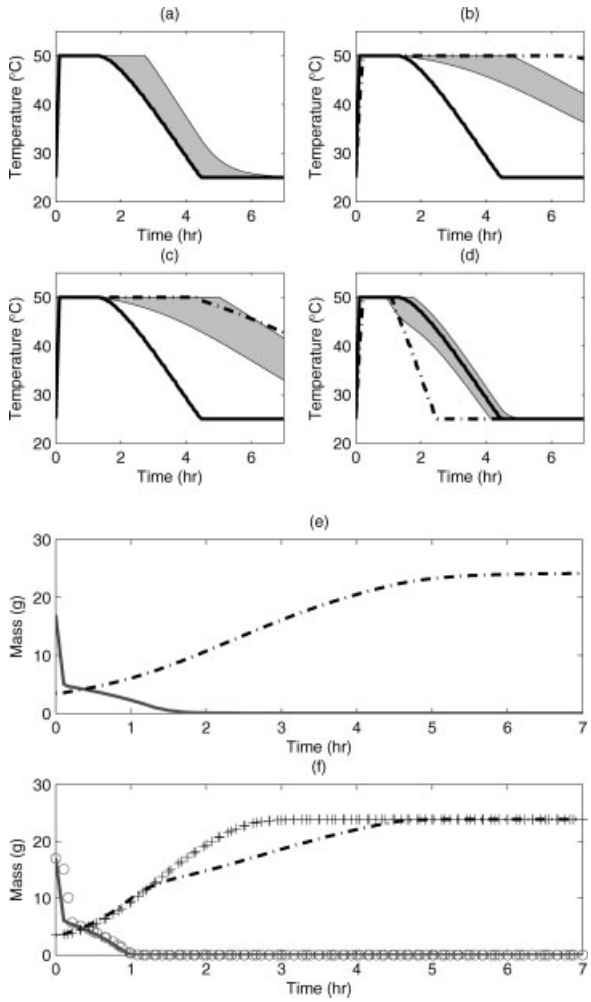

Figure 3. Temperature profiles applied to: (a) case 1, (b) case 2, (c) case 3, and (d) case 4, for T-control (−), the temperature trajectory reoptimized for the perturbed model parameters (− · − ·), and the shaded region showing the constraints on the temperature for T-control.

Mass profiles for: (e) case 1 and (f) case 4, for T-control (M_α, −; M_β, − · − ·), and for the temperature trajectory reoptimized for the perturbed model parameters (M_α, ○; M_β, +). (The mass profiles for cases 2 and 3 are not shown since the temperature trajectories do not satisfy the operating constraints).

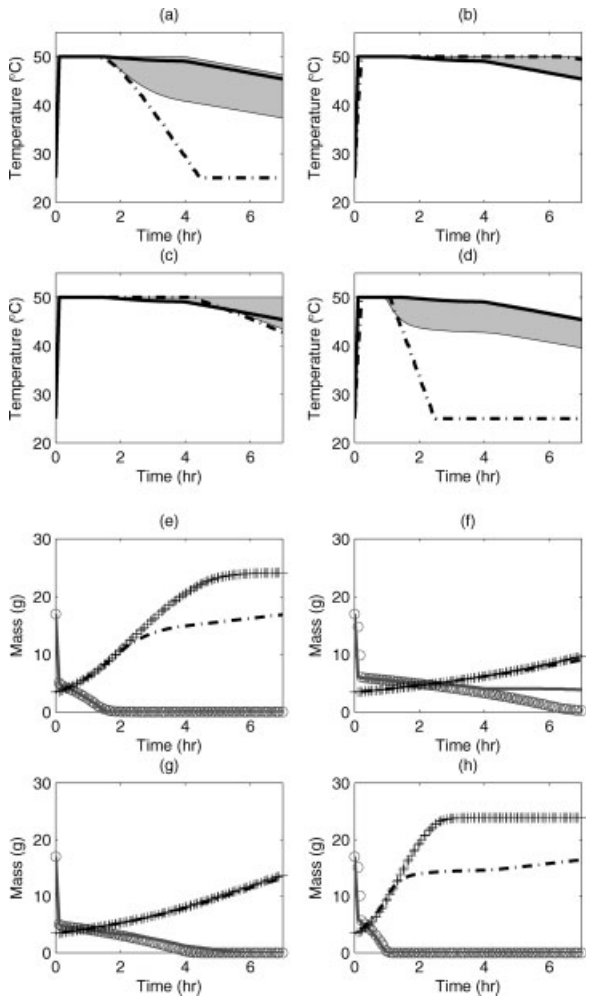

Figure 4. Temperature profiles applied to: (a) case 1, (b) case 2, (c) case 3, and (d) case 4, for robust T-control (−), the temperature trajectory reoptimized for the perturbed model parameters (− · − ·), and the shaded region showing the constraints on the temperature for robust T-control.

Mass profiles for: (e) case 1, (f) case 2, (g) case 3, and (h) case 4, for robust T-control (M_α, −; M_β, − · − ·), and for the temperature trajectory reoptimized for the perturbed model parameters (M_α, ○; M_β, +).

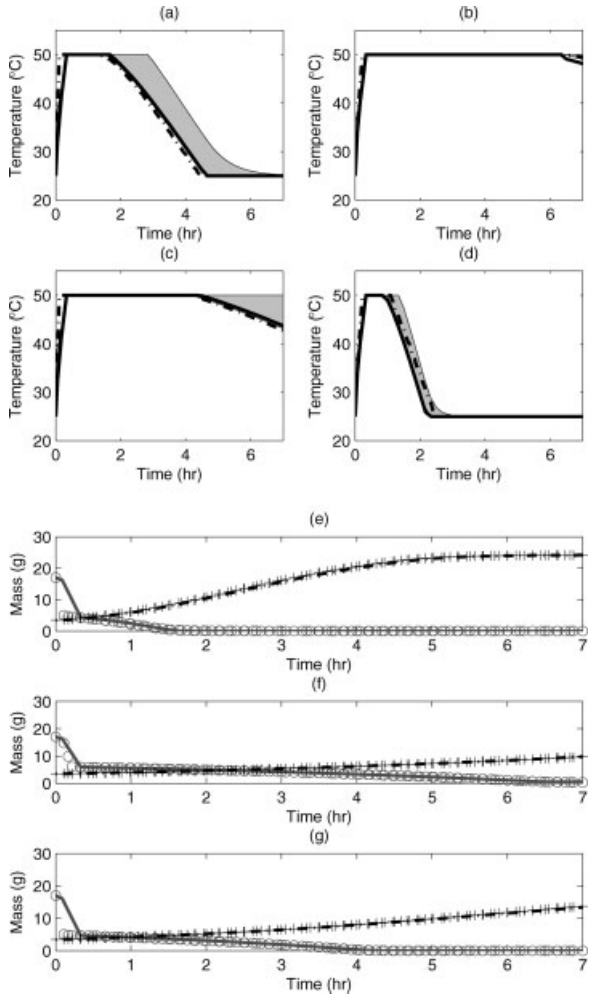

Figure 5. Temperature profiles applied to (a) case 1, (b) case 2, (c) case 3, and (d) case 4, for C-control (−), the temperature trajectory reoptimized for the perturbed model parameters (− · − ·), and the shaded region showing the constraints on the temperature for C-control.

Mass profiles for: (e) case 1, (f) case 2, and (g) case 3, for C-control (M_α, −; M_β, − · − ·), and for the temperature trajectory reoptimized for the perturbed model parameters (M_α, ○; M_β, +). (The mass profiles for case 4 are not shown since the temperature trajectory (slightly) violates the T lower limit).

trol without having the poor robustness of T-control computed from the nominal model. In summary, C-control has all the respective advantages of T-control and robust T-control, without any of their respective disadvantages.

C-control uses nonlinear state feedback control of the concentration measurement to follow a desired path in the phase diagram.[26] This article, for the first time, demonstrates the improved robustness of C-control for the solvent-mediated transformation from one polymorph to another. There is theoretical and simulation support that relatively simple nonlinear state feedback controllers can be derived that provide nearly optimal performance and robustness for batch processes.[16] For a polymorphic crystallization, this paper derives such a nonlinear state feedback controller, motivated by and interpreted within the context of the crystallization phase diagram, which has the desired performance and robustness properties.

Conclusions

The robustness and performance of T-control, robust T-control, and C-control strategies were compared for maximizing the batch productivity during the solvent-mediated polymorphic transformation of L-glutamic acid from the metastable α-form to the stable β-form crystals. Operating a batch polymorphic crystallization using the existing approach based on control along a temperature vs. time trajectory[21] is shown to be very sensitive to variations in the nucleation and growth kinetics and shifts in the solubility curve, resulting in violations of the operating constraints. For the polymorphic transformation from α-form to β-form crystals, these constraint violations can result in the nucleation and re-growth of undesired α-form crystals. Robust T-control resulted in satisfaction of the operating constraints for a full range of variations in the physicochemical parameters for the kinetics and thermodynamics of the polymorphic transformation, but resulted in very poor batch productivity (long batch times) for parameters in which short batch times are possible.

A nonlinear state feedback controller designed to follow an optimal trajectory in the concentration-vs-temperature-

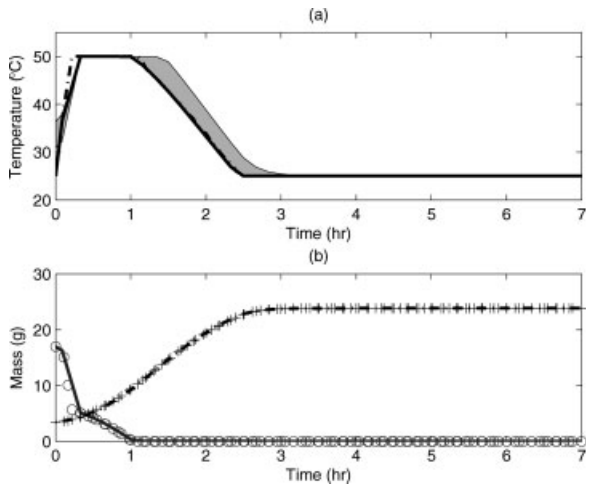

Figure 6. (a) Temperature profile applied to case 4 for C-control with parameters p_1 = 36.56, p_2 = 11.5, p_3 = 0.4185, and p_4 = 0.03656 (−), the temperature trajectory reoptimized for the perturbed model parameters (− · − ·), and the shaded region showing the constraints on the temperature for C-control; (b) the corresponding mass profiles for C-control (M_α, −; M_β, − · − ·), and for the temperature trajectory reoptimized for the perturbed model parameters (M_α, ○; M_β, +).

phase diagram was highly robust to variations in the kinetic parameters, while providing batch productivity nearly as high as optimal control applied to batch crystallization with known parameters, as illustrated in Figure 5c,g and many simulation studies (not shown here) with variations in θ_1 to θ_3 (while maintaining $\theta_4 = \theta_5 = 0$). Although not explicitly included in the optimization formulation, the operating constraints were satisfied for the entire range of physicochemical parameters (see Figure 5), except for a small constraint violation due to variation in the solubility of α-form crystals that was removed by slightly shifting the concentration setpoint trajectory away from the α-solubility curve (Figure 6). Alternatively, shifts in any solubility curve can be accounted for by updating measurements of the solubility curve whenever there are significant changes in feedstocks between batch runs. Automated systems exist for measuring such solubility curves.[17,19,26]

Published results,[2,20] as well as one of the author's experience consulting with industry on their polymorphic crystallizations suggest that the solubility curves of most polymorphs are typically much closer together than for the α and β polymorphs of L-glutamic acid (Figure 1).[§] If this is true, then the desired operating region for most polymorphic crystallizations is typically much smaller than for the system investigated in this study, making the robustness of batch control strategies of much greater importance for most polymorphic crystallizations. The results in this article indicate that the design of operating procedures for future polymorphic crystallizations should implement C-control.

Literature Cited

1. De Anda JC, Wang XZ, Lai X, Roberts KJ. Classifying organic crystals via in-process image analysis and the use of monitoring charts to follow polymorphic and morphological changes. *J Process Contr*. 2005;15:785–797.
2. Blagden N, Davey R. Polymorphs take shape. *Chem Brit*. 1999;35:44–47.
3. Fujiwara M, Nagy ZK, Chew JW, Braatz RD. First-principles and direct design approaches for the control of pharmaceutical crystallization. *J Process Contr*. 2005;15:493–504.
4. Rohani S, Horne S, Murthy K. Control of product quality in batch crystallization of pharmaceuticals and fine chemicals. Part 1: Design of the crystallization process and the effect of solvent. *Org Process Res Dev*. 2005;9:858–872.
5. Yu LX, Lionberger RA, Raw AS, D'Costa R, Wu HQ, Hussain AS. Applications of process analytical technology to crystallization processes. *Adv Drug Delivery Rev*. 2004;56:349–369.
6. Cardew PT, Davey RJ. The kinetics of solvent-mediated phase transformations. *Proc R Soc Lond A*. 1985;398:415–428.
7. Hu Q, Rohani S, Jutan A. Modelling and optimization of seeded batch crystallizers. *Comput Chem Eng*. 2005;29:911–918.
8. Larsen PA, Patience DB, Rawlings JB. Industrial crystallization process control. *IEEE Contr Syst Mag*. 2006;26:70–80.
9. Rawlings JB, Miller SM, Witkowski WR. Model identification and control of solution crystallization processes: *A review*. *Ind Eng Chem Res*. 1993;32:1275–1296.
10. Worlitschek J, Mazzotti M. Model-based optimization of particle size distribution in batch-cooling crystallization of paracetamol. *Cryst Growth Des*. 2004;4:891–903.
11. Zhang GP, Rohani S. On-line optimal control of a seeded batch cooling crystallizer. *Chem Eng Sci*. 2003;58:1887–1896.
12. vvBraatz RD, Fujiwara M, Wubben T, Rusli E. Crystallization: Particle size control. In: Swarbrick J, editor. *Encyclopedia of Pharmaceutical Technology,* 3rd ed. New York: Marcel Dekker, 2006:858–871 (invited).
13. Rohani S, Horne S, Murthy K. Control of product quality in batch crystallization of pharmaceuticals and fine chemicals. Part 2: External control. *Org Process Res Dev*. 2005;9:873–883.
14. Diehl M, Bock HG, Kostina E. An approximation technique for robust nonlinear optimization. *Math Program Ser B*. 2006;107:213–230.
15. Ma DL, Braatz RD. Worst-case analysis of finite-time control policies. *IEEE Trans Contr Syst Technol*. 2001;9:766–774.
16. Srinivasan B, Bonvin D, Visser E, Palanki S. Dynamic optimization of batch processes – II. Role of measurements in handling uncertainty. *Comput Chem Eng*. 2003;27:27–44.
17. Fujiwara M, Chow PS, Ma DL, Braatz RD. Paracetamol crystallization using laser backscattering and ATR-FTIR spectroscopy: Metastability, agglomeration and control. *Cryst Growth Des*. 2002;2:363–370.
18. Gron H, Borissova A, Roberts KJ. In-process ATR-FTIR spectroscopy for closed-loop supersaturation control of a batch crystallizer producing monosodium glutamate crystals of defined size. *Ind Eng Chem Res*. 2003;42:198–206.
19. Liotta V, Sabesan V. Monitoring and feedback control of supersaturation using ATR-FTIR to produce an active pharmaceutical ingredient of a desired crystal size. *Org Process Res Dev*. 2004;8:488–494.
20. Brittain HG. The impact of polymorphism on drug development: A regulatory viewpoint. *Am Pharmaceut Rev*. 2000;3:67–70.
21. Ono T, Kramer HJM, Ter Horst JH, Jansens PJ. Process modeling of the polymorphic transformation of L-glutamic acid. *Cryst Growth Des*. 2004;4:1161–1167.
22. Miller SM, Rawlings JB. Model identification and control strategies for batch cooling crystallizers. *AIChE J* 1994;40:1312–1327.
23. Nagy ZK, Braatz RD. Worst-case and distributional robustness analysis of finite-time control trajectories for nonlinear distributed parameter systems. *IEEE Trans Contr Syst Technol*. 2003;11:694–704.
24. Hu Q, Rohani S, Wang DX, Jutan A. Optimal control of a batch cooling seeded crystallizer. *Powder Technol*. 2005;156:170–176.
25. Matthews HB, Rawlings JB. Batch crystallization of a photochemical: Modeling, control, and filtration. *AIChE J*. 1998;44:1119–1127.
26. Zhou GX, Fujiwara M, Woo XY, Rusli E, Tung HH, Starbuck C, Davidson O, Ge Z, Braatz RD. Direct design of pharmaceutical antisolvent crystallization through concentration control. *Cryst Growth Des*. 2006;6:892–898.
27. Kee N, Woo XY, Goh L, Chen K, He G, Bhamidi V, Rusli E, Nagy ZK, Kenis PJA, Zukoski CF, Tan RBH, Braatz RD. Design of crystallization processes from laboratory R&D to the manufacturing scale. *Am Pharmaceut Rev*. 2008;11:to appear.
28. Seborg DE, Henson MA. *Nonlinear Process Control*. 1st ed. Piscataway, NJ: Prentice Hall; 1996.
29. Togkalidou T, Fujiwara M, Patel S, Braatz RD. Solute concentration prediction using chemometrics and ATR-FTIR spectroscopy. *J Cryst Growth*. 2001;231:534–543.

Manuscript received Nov. 14, 2006, and final revision received May 31, 2007.

[§]This is especially true for enantiomeric polymorphs, in which the solubility curves intersect.